Release of ^{37}K from catcher foils

D. Melconian[a], M. Trinczek[b,1], A. Gorelov[a], W.P. Alford[c], J.A. Behr[d,*],
J.M. D'Auria[b], M. Dombsky[d], U. Giesen[d,e,2], K.P. Jackson[d],
T.B. Swanson[a,3], W. Wong[d]

[a]*Department of Physics, Simon Fraser University, 8888 University Drive, Burnaby, BC, Canada V5A 1S6*
[b]*Department of Chemistry, Simon Fraser University, 8888 University Drive, Burnaby, BC, Canada V5A 1S6*
[c]*Department of Physics, University of Western Ontario, London, Ont., Canada*
[d]*TRIUMF, 4004 Wesbrook Mall, Vancouver, BC, Canada V6T 2A3*
[e]*Department of Physics, University of Alberta, Edmonton, Alta., Canada T6G 2JA*

Abstract

The release fraction of implanted 12 keV ^{37}K ($T_{1/2} = 1.23$ s) ions from a variety of catcher foils was measured. The temperature dependence was measured for V, Fe, Ni, Y, Zr, Nb, Mo, Hf, Ta, W, Re, C, and Pt foils. The release fraction was found empirically to be a reasonably universal function of the ratio of temperature to catcher melting point. Limits on diffusion parameters (ignoring desorption) and on desorption (ignoring diffusion) were deduced. The results were used to find the optimal neutralizing catcher foil to load a neutral atom trap, and can be used to help choose ISOL target production materials.

© 2004 Elsevier B.V. All rights reserved.

PACS: 66.30; 34.50.Dy; 81.15.J; 68.43; 32.80.Pj

Keywords: Diffusion; Desorption; Ion; Atom trap; Neutralization

1. Introduction

Neutral atom traps for alkali atoms with radioactive isotopes [1] are often loaded from mass-separated low-energy ion beams stopped in foils [2–4]. For atoms with half-lives of the order of a second, similarly short release times from the neutralizing material are needed to optimize loading efficiency. The vapor cell magneto-optical

*Corresponding author.

 E-mail address: behr@triumf.ca (J.A. Behr).

[1]Present address: TRIUMF, 4004 Wesbrook Mall, Vancouver, BC, Canada V6T 2A3.

[2]Present address: Physikalisch-Technische Bundesanstalt, 38116 Braunschweig, Germany.

[3]Present address: US Naval Observatory, 3450 Massachusetts Avenue, NW, Washington, DC 20392, USA.

trap [5] must exist in close proximity to the catcher, so a catcher with relatively low temperature and vapor pressure is needed. In addition, production of the radioactive alkalis at on-line isotope separators depends on release of the alkali metals from the production target. Therefore, we have surveyed release of ^{37}K from various materials.

An empirical result of the survey is that the release fraction is a reasonably universal function of the ratio of catcher temperature to catcher melting point. Significant release of the short-lived ^{37}K isotope occurred at about half the melting point of each material. We qualitatively discuss this result in terms of semiempirical relations for diffusion and desorption.

Our method does not distinguish between diffusion, which describes an atom's transport through the bulk of a material, and desorption, which is the mechanism by which an atom escapes from the surface of a material. We parameterize the results using simple expressions describing diffusion. Our diffusion parameters should be regarded as upper limits for the time of diffusion, because desorption could very well be an important source of delay times for release. We also fit our data to expressions for pure desorption, and these can similarly be interpreted as upper limits for the time of desorption. We compare our experimental results to diffusion and desorption parameters from the literature for four cases.

2. Experiment

The on-line isotope separator TISOL [6] was used to make a clean mass-separated 12 keV ^{37}K beam. The beam was continuously implanted in the catcher foil (see Fig. 1), and the fraction of implanted ^{37}K atoms remaining in the sample was measured as a function of the sample temperature. The fraction released is precisely the quantity of interest for loading the neutral atom trap.

To monitor the sample activity, the sample was mounted in front of a thick aluminum positron stopper. The stopper subtended approximately 40% of the solid angle for escaping positrons. Two 5×5 cm NaI(Tl) scintillator detectors were
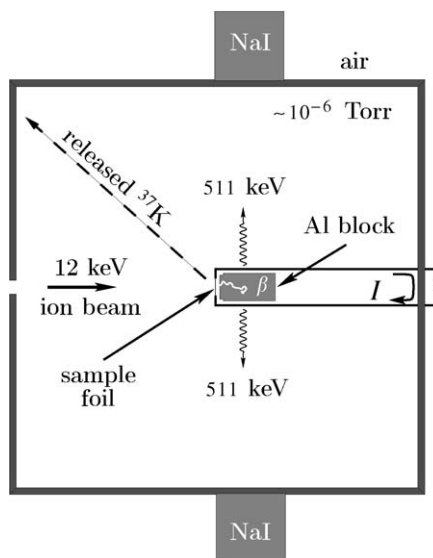

Fig. 1. Schematic diagram of the experimental setup. Positrons from ^{37}K decay are stopped in the aluminum block. Their annihilation radiation is detected in coincidence to localize the ^{37}K activity and determine whether or not the ^{37}K has remained in the foil as it is heated by direct current I.

placed back-to-back 15 cm away from the stopper. The coincidence rate in the two detectors, which was dominated by decays of positrons from the stopper, was monitored as a function of sample temperature. When ^{37}K escaped from the sample into the 30×30 cm chamber, the positrons from its decays were no longer stopped in the stopper. So the coincidence rate is directly proportional to the number of ^{37}K atoms remaining in the sample, and the fraction remaining is equal to one minus the release fraction. A correction of typically 5% for accidental coincidences was made, measured by the standard technique of delaying one detector signal to eliminate true coincidences.

The sample was heated by direct current, and the temperature measured with an optical pyrometer. The beam spot size was approximately 6 mm, and the foil width was 1.5 cm, so the temperature was uniform across the activity region. The vacuum in this test setup was 2×10^{-6} Torr, so the testing times were kept short to avoid foil contamination such as oxidation. The results shown here were reproducible and showed no signs of degradation for the short testing times

used, although we found that foils tested for longer times at poorer vacuum certainly show signs of degradation. In practice, release of ^{37}K at 2×10^{-9} Torr is achieved from Zr in our neutral-atom trap for months without degradation of the foil's release or neutralization efficiency.

2.1. Lower temperature melting point materials

We comment briefly on unsuccessful attempts to find catchers with efficient release at lower temperatures. The high temperatures needed for release are detrimental to the neutral-atom trap for at least two reasons. The most obvious is the potential for damage to the silicon-based polymer ("Dryfilm") [7] coatings of the vapor cell to which the alkalis do not stick, either by heating of the coatings or evaporation of the catcher material and its impurities. In addition, the higher average velocity of the atoms will reduce the fraction captured on the first pass through the laser beams, and could also increase the rate of permanent chemical bonding on the first impact with the vapor cell.

Semiempirical expressions exist [8] which relate the enthalpy of adsorption to bulk properties of materials, such as their melting points and work functions. Guided by these, we have searched for release from materials with much lower melting points. As one approaches the melting point of a material, diffusion can be expected to almost always increase to the point where fast diffusion can be achieved, and the limitation would be expected to be the rate of desorption. Aluminum, indium, and lithium were tried. The lithium was prepared by scraping the final surface under an argon atmosphere. Aluminum and indium are materials with very low vapor pressures near their melting points. Lithium is an alkali metal and would not be expected to stick permanently to Dryfilm coatings, and might also cure Dryfilm defects, as occurs with other alkalis [5]. However, no significant release was seen from these three materials up to their melting points. We suspect that this is most likely due to surface contamination.

3. Diffusion phenomenology

Ignoring desorption, we treat the release of impurities from the host using Fick's law for diffusion, $J_n = -D\nabla n$, which relates the flux, J_n, of atoms in a material to the gradient of their concentration, n. The diffusion constant D for solids is described by an Arrhenius relation $D = D_0 \exp(-E_a/kT)$, where D_0 is a phenomenological 'frequency factor' and E_a is an activation energy. The beam used was ≈ 0.6 cm diameter, and implantation depths are ~ 100 Å, so it is appropriate to use one-dimensional expressions and solutions.

For a semi-infinite slab, the method of image charges yields the general solution [9,10] for the time and spatial dependence of the distribution of impurities with radioactive lifetime τ:

$$N(x,t) = \frac{\exp(-t/\tau)}{2\sqrt{\pi D t}} \int_0^\infty n_0(\xi) \left[\exp\left(\frac{(x-\xi)^2}{4Dt}\right) - \exp\left(\frac{(x+\xi)^2}{4Dt}\right) \right] \mathrm{d}\xi. \tag{1}$$

We use the code TRIM [11] to calculate the initial implantation distribution $n_0(\xi)$. Some of the implantation distributions can be modelled by a Gaussian times a linear term in terms of a characteristic implantation depth d,

$$n_0(x) = \frac{4N_0}{\sqrt{\pi}d} \left(\frac{x}{d}\right) \exp(-x^2/d^2) \tag{2}$$

and, integrating over the material, the result has an analytic expression for the atoms remaining as a function of time [12]:

$$N(t) = \frac{N_0}{\sqrt{1 + 4Dt/d^2}} \exp(-t/\tau). \tag{3}$$

Integrating over time gives $1 - F$, with the release fraction, F, given by

$$F = 1 - \sqrt{\frac{\pi}{4\alpha}} \exp\left(\frac{1}{4\alpha}\right) \left(1 - \mathrm{erf}\left(\sqrt{\frac{1}{4\alpha}}\right)\right) \tag{4}$$

where the parameter $\alpha = \tau D/d^2$. Although it is not readily apparent, this function is well-behaved, but the divergence of its separate terms makes its numerical evaluation for small values of α difficult.

A less accurate but more generally applicable expression that is somewhat simpler to use is given by Liatard et al. [9]:

$$F = \exp\left(-\frac{1}{\sqrt{\alpha}}\right)\frac{\sinh(f/\sqrt{\alpha})}{f/\sqrt{\alpha}} \tag{5}$$

for a finite flat-topped distribution of mean implantation depth d and one sigma depth straggling σ, with the parameter $f = \sigma/d$. The fit values from either expression agree within our errors, and we use Eq. (5) to extract diffusion parameters from our data.

Although it is customary to quote D_0 as a parameter, it is well-known that when extrapolating to infinite temperature to determine D_0, small uncertainties in E_a produce larger errors in D_0 than are inherent in the data. We therefore also parameterize (as in Ref. [12]) in terms of a constant D_{1200} that better characterizes diffusion in the temperatures in the range measured:

$$D_{1200} = D_0 \exp\left(-\frac{E_a}{k(1200\,\text{K})}\right). \tag{6}$$

3.1. Desorption fits

We also fit to an expression assuming pure desorption with no diffusion, $F = \mu(\mu + \lambda)^{-1}$ [13], where λ is the radioactive decay rate and μ obeys an Arrhenius relation $\mu = C \exp(-E_d/kT)$, with E_d the desorption energy.

4. Results

Typical experimental data for each foil are shown in Fig. 2, along with the results of the fits to Eq. (5). There are no clear trends as a function of lattice type.

The activation energy for self-diffusion of elements is known to be related to their melting point [14]. In addition, the semiempirical relations for enthalpies of desorption in Ref. [8] depend on the melting point of the material. So we also plot, in Fig. 3, the results as a function of T/T_{melt} for each material. It is remarkable that materials with release temperatures differing by a factor of two all
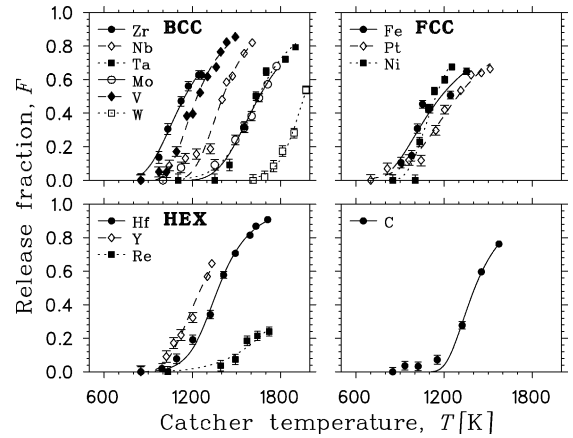

Fig. 2. Release fraction as a function of temperature, grouped by lattice type. Experimental results and the best fits using Eq. (5) are shown. Upper left is body-centered cubic (BCC), upper right is face-centered cubic (FCC), lower left is hexagonal close-packed (HEX), lower right is carbon, which was in the form of pyrolytic graphite.
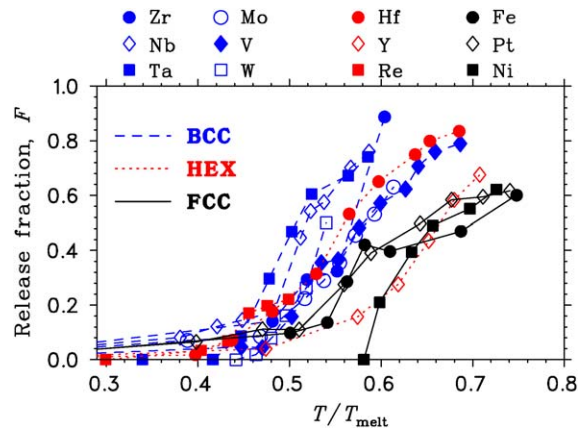

Fig. 3. Experimental results for release of ^{37}K from various foils, plotted as a function of the ratio of the foil temperature, T, to its melting point, T_{melt}. Lines connect the data and are shown to guide the eye. The qualitative result is that all materials show substantial release at about half their melting point. Carbon, which does not melt and so is not plotted, releases half of the atoms at a temperature 0.32 times its vaporization temperature.

cluster together to within approximately 15% as a function of T/T_{melt}. Apparently, parameterization by T/T_{melt} can be used phenomenologically to estimate release times from catchers. Note also that there appears to be some dependence on

lattice type, as the FCC lattice requires temperatures closer to its melting point to achieve finite release, but the small sample size means that no quantitative conclusions can be drawn.

The utility of this parameterization in terms of T/T_{melt}, as well as similar dependence on BCC and FCC lattice type, was observed in the diffusion of ^{23}Na [15]. Calculations of the dependence of diffusion on lattice type date at least to the classic paper of Wert [16]. For a recent review, see Ref. [17], and see Ref. [18] for an example of recent work.

The fit results are also listed in Table 1 for both the diffusion parameters from Eq. (5) and the desorption parameters in the expressions of Section 3.1. There is no direct information in our data, nor in the the quality of the fits, to determine whether diffusion or desorption dominates any particular case. So the diffusion rates deduced from these parameters should be regarded as upper limits on the diffusion process, as we assume desorption times are negligible for those fits. Similarly, desorption rates derived from these parameters should be

treated as upper limits on desorption rates, because they ignore diffusion.

5. Discussion

For our purposes, zirconium was chosen as a catcher foil. Zirconium has release times similar to those of yttrium, which is widely used for this purpose [19], but zirconium has a vapor pressure that is lower by four orders of magnitude. Although its work function ($\sim$4.0 eV) is not as low as that of yttrium, it is low enough to release most of the potassium (ionization energy 4.34 eV) as neutral atoms rather than surface-ionized ions. We have determined the neutral fraction to be greater than 80% by applying a bias between a nearby collimator and the foil and noting that the release did not change. We are able to use this catcher for loading our neutral atom trap with ^{37}K for 4–8 weeks before the Dryfilm coating is degraded.

We have also attempted to observe hysteresis curves for the two cases we measured that have

Table 1
Parameters from the diffusion fits and from the desorption fits

Foil	E_a (eV)	D_0 (cm²/s)	D_{1200} (cm²/s)	C (s⁻¹)	E_d (eV)
αZr	1.18 ± 0.09	$1.5^{+2.2}_{-1.3} \times 10^{-7}$	$1.67^{+0.15}_{-0.14} \times 10^{-12}$	3.8×10^3	0.91 ± 0.16
βZr	1.41 ± 0.15	$1.8^{+7.8}_{-1.5} \times 10^{-6}$	$2.29^{+0.52}_{-0.42} \times 10^{-12}$	1.4×10^4	0.99 ± 0.14
Hf	2.46 ± 0.10	$4.4^{+9.0}_{-0.34} \times 10^{-4}$	$2.11^{+0.48}_{-0.40} \times 10^{-12}$	6.1×10^4	1.38 ± 0.05
Y	1.59 ± 0.15	$4.7^{+17}_{-3.5} \times 10^{-6}$	$9.7^{+1.2}_{-1.1} \times 10^{-13}$	1.8×10^4	1.13 ± 0.08
C	2.19 ± 0.18	$1.2^{+5.2}_{-1.0} \times 10^{-4}$	$7.6^{+3.2}_{-2.3} \times 10^{-14}$	9.4×10^4	1.46 ± 0.09
Re	1.84 ± 0.43	$8^{+150}_{-8} \times 10^{-9}$	$1.5^{+2.5}_{-1.0} \times 10^{-16}$	3.2×10^2	1.09 ± 0.24
Ta	2.81 ± 0.28	$1.1^{+6.3}_{-0.9} \times 10^{-4}$	$1.8^{+1.9}_{-1.0} \times 10^{-16}$	5.0×10^4	1.62 ± 0.17
Fe	0.80 ± 0.13	$1.3^{+3.6}_{-0.9} \times 10^{-9}$	$5.5^{+1.2}_{-0.9} \times 10^{-13}$	9.1×10^1	0.52 ± 0.09
V	1.76 ± 0.09	$1.2^{+1.7}_{-0.7} \times 10^{-5}$	$4.89^{+0.52}_{-0.48} \times 10^{-13}$	2.5×10^4	1.15 ± 0.05
Pt	1.10 ± 0.09	$3.8^{+4.7}_{-2.0} \times 10^{-9}$	$8.8^{+1.1}_{-1.0} \times 10^{-14}$	1.9×10^2	0.65 ± 0.06
Mo	2.39 ± 0.20	$8.1^{+28}_{-6.1} \times 10^{-6}$	$7.6^{+5.3}_{-3.2} \times 10^{-16}$	3.2×10^4	1.57 ± 0.10
Ni	1.60 ± 0.25	$4.3^{+52}_{-3.9} \times 10^{-6}$	$8.5^{+2.2}_{-1.7} \times 10^{-13}$	2.3×10^4	1.05 ± 0.20
Nb	2.52 ± 0.27	$5.7^{+24}_{-5.7} \times 10^{-4}$	$1.6^{+2.4}_{-0.8} \times 10^{-14}$	1.7×10^5	1.54 ± 0.14
W	6.1 ± 1.1	$9.3^{+28}_{-9.3} \times 10^{+2}$	$2.7^{+14}_{-2.3} \times 10^{-23}$	1.1×10^9	3.62 ± 0.26

The parameter D_{1200}, which is defined in Eq. (6), provides a better description of the diffusion process in our temperature region than D_0. Diffusion coefficients D computed from these parameters should be treated as upper limits (because they ignore desorption) and desorption rates computed from these parameters should also be treated as upper limits (because they ignore diffusion). αZr includes points above its phase transition, βZr does not. Comparison to literature diffusion data for Mo, Fe, and Nb and desorption data for Mo, Nb, Ta suggest that release from these foils has contributions from both processes (see text).

known phase transitions, zirconium and iron. In the case of zirconium, there is a dramatic increase in diffusion rate at its known HEX to BCC phase transition at $863\,^\circ$C, but the hysteresis effects were found to be difficult to quantify. We include in the table two fits, either including or not including points at temperatures higher than the phase transition. These fits show a suggestive but not conclusive difference in diffusion and desorption constants.

The parameters describing tungsten release appear to be quite different from the others. We note that the tungsten release fraction data does have a qualitatively steeper dependence on temperature than, for example, the rhenium data, so a larger E_a or E_d is indeed necessary.

5.1. Comparison to data in the literature

There are measurements in the literature [20] of ^{42}K diffusion in three of the materials measured here, Mo ($E_a = 1.08\,$eV, $D_0 = 5.5 \times 10^{-9}\,$cm^2/s) [21], Nb (0.95 eV, $2.38 \times 10^{-7}\,$cm^2/s) [21], and αFe (1.83 eV, $0.036\,$cm^2/s) [22], with no errors listed. If we use these parameters and Eq. (5), then much faster release is predicted than we observed experimentally. Our data would imply that each of these three foils must be heated to temperatures that are 400–500° higher in order to achieve similar release rates. This suggests that even in our simple geometry the release from Mo, Fe, and Nb foils has a strong contribution from desorption.

In addition, Kirchner measured values of E_d of approximately 3.4 eV for potassium desorption from Ta, Mo, and Nb [23], although the phenomenological equivalent of C was not reported. By combining these results with the above diffusion data, we can compare more directly to the literature for Mo and Nb.

The functional form of the release fraction when both diffusion and desorption are present is the product of the individual release fractions for pure diffusion and pure desorption [23]. If for Mo and Nb we fix E_a and E_d to be the values from the literature, then we are able to fit for D_0 and C, and the fits are of similar quality to those using either pure expression. For Mo, the fit $D_0 = (1.5 \pm$

0.5$) \times 10^{-9}\,$cm^2/s, and $C = (1.0 \pm 0.7) \times 10^{11}\,$s^{-1}, although our error on D_0 is made artificially low by fixing E_a exactly. Although it is difficult to draw quantitative conclusions, order-of-magnitude agreement on D_0 is satisfactory given the large inherent errors on this quantity. For Nb, the fit $D_0 = (6.7 \pm 3.2) \times 10^{-9}\,$cm^2/s and $C = (1.9 \pm 0.9) \times 10^{12}\,$s^{-1}, and the value for D_0 is in greater disagreement with the literature, again with no errors given.

We can also attempt to extract desorption information for Fe by fixing D_0 and E_a to the values above. Then our fit desorption results are $E_d = 0.48 \pm 0.09\,$eV and $C = 65 \pm 62\,$s^{-1}, and the value of E_d does not change significantly from our fit containing desorption alone. This implies that the release from Fe is dominated by desorption.

By letting all parameters float for Ta, we find fit parameters $E_a = 1.44 \pm 0.88\,$eV, $D_0 = 2^{+18}_{-2} \times 10^{-8}\,$cm^2/s, $E_d = 3.4 \pm 0.8\,$eV, and $C = 7^{+55}_{-7} \times 10^{11}\,$s^{-1}, and the confidence level of the fit improves from 0.1% to 59%. The desorption energy E_d agrees with Ref. [23], which lends credibility to the diffusion parameters extracted, albeit with large fit uncertainties.

In summary, despite the unknown errors on the literature values, we regard the level of disagreement between the literature and our fit value of D_0 with E_a and E_d fixed to be satisfactory for Mo and Nb, given the inherently large error in the determination of D_0. We are able to extract diffusion parameters in the presence of desorption for Ta, and desorption parameters in the presence of diffusion for Fe. The differences in these diffusion and desorption parameters from those in Table 1 illustrate the difficulty in extracting useful physical information about either process from our fits to diffusion or desorption alone for the other cases. Nevertheless, our fit parameters can be used phenomenologically as limits for either process.

6. Summary

We have investigated a wide variety of catcher foils to load a magneto-optical trap with short-lived potassium isotopes. Our main phenomen-

ological result, summarized in Fig. 3, is that all foils tested release at least half of a 1 s half-life potassium isotope when heated to a temperature between 0.45 and 0.6 of their melting point.

Acknowledgements

References

[1] J.A. Behr, Nucl. Instr. and Meth. B 204 (2003) 526.

[2] M. Trinczek, A. Gorelov, D. Melconian, W.P. Alford, D. Asgeirsson, D. Ashery, J.A. Behr, P.G. Bricault, J.M. D'Auria, J. Deutsch, J. Dilling, M. Dombsky, P. Dube', S. Eaton, J. Fingler, U. Giesen, S. Gu, O. Häusser, K.P. Jackson, B. Lee, J.H. Schmid, T.J. Stocki, T.B. Swanson, W. Wong, Phys. Rev. Lett. 90 (2003) 012501.

[3] S.G. Crane, S.J. Brice, A. Goldschmidt, R. Guckert, A. Hime, J.J. Kitten, D.J. Vieira, X. Zhao, Phys. Rev. Lett. 86 (2001) 2967.

[4] J.M. Grossman, L.A. Orozco, M.R. Pearson, J.E. Simsarian, G.D. Sprouse, W.Z. Zhao, Phys. Rev. Lett. 83 (1999) 935.

[5] M. Stephens, C. Wieman, Phys. Rev. Lett. 72 (1994) 3787; M. Stephens, R. Rhodes, C. Wieman, J. Appl. Phys. 76 (1994) 3479.

[6] J.M. D'Auria, J. Behr, L. Buchmann, M. Dombsky, K.P. Jackson, H. Sprenger, Nucl. Instr. and Meth. B 126 (1997) 7.

[7] D.R. Swenson, L.W. Anderson, Nucl. Instr. and Meth. B 29 (1988) 627.

[8] A.R. Miedema, J.W.F. Dorleijn, Surf. Sci. 95 (1980) 447.

[9] E. Liatard, G. Gimond, G. Perrin, F. Schussler, Nucl. Instr. and Meth. A 385 (1997) 198.

[10] H.S. Carslaw, J.C. Jaeger, Conduction of Heat in Solids, second ed., Clarendon Press, Oxford, 1992; J. Crank, The Mathematics of Diffusion, second ed., Clarendon Press, Oxford, 1975.

[11] J.F. Ziegler, J.P. Biersack, U. Littmark, The Stopping Ranges of Ions in Matter, vol. 1. Pergamon Press, Toronto, calculations were performed with SRIM-2003 version 26 (see www.SRIM.org), 1985.

[12] T. Warner, G. Ball, J.A. Behr, T.E. Chupp, P. Finlay, G. Hackman, B. Hyland, K. Koopmans, S.R. Nuss-Warren, A.A. Phillips, M.A. Schumaker, C.E. Svensson, E.R. Tardiff, P. Finlay, Nucl. Instr. and Meth. A, in press.

[13] H.L. Ravn, Phys. Rep. 54 (1979) 201.

[14] See, e.g., R.J. Borg, G.J. Dienes, An Introduction to Solid-State Diffusion, Academic Press Inc., Boston, 1988.

[15] M. Uhrmacher, K.P. Lieb, Nucl. Instr. and Meth. B 68 (1992) 175.

[16] C.A. Wert, Phys. Rev. 79 (1950) 601.

[17] M.E. Glicksman, Diffusion in Solids: Field Theory, Solid-State Principles, and Applications, Wiley, New York, 2000.

[18] N.P. Lazarev, A.S. Bakai, C. Abromeit, V. Naundorf, Phys. Rev. Lett. 88 (2002) 045502.

[19] See, e.g., C. Ekstrom, L. Robertsson, A. Rosen, Physica Scripta 34 (1986) 624; C. Thibault, P. Guimbal, R. Klapisch, M. de Saint Simon, J.M. Serre, F. Touchard, S. Buttgenbach, H.T. Duong, P. Jacquinot, P. Juncar, S. Liberman, P. Pillet, J. Pinard, J.L. Vialle, G. Huber, A. Pesnelle, Nucl. Instr. and Meth. 186 (1981) 193; R. Guckert, X. Zhao, S.G. Crane, A. Hime, W.A. Taylor, D. Tupa, D.J. Vieira, H. Wollnik, Phys. Rev. A 58 (1998) R1637; and, Ref. [4].

[20] D.R. Lide (Ed.), Handbook of Chemistry and Physics, 1991, Chemical Rubber Company, evaluated by John Askill from John Askill, Tracer Diffusion Data for Metals, Alloys and Simple Oxides, Plenum Press, New York, 1970.

[21] G.N. Dubinin, G.P. Benediktova, M.G. Karpman, G.V. Shcherbedinskii, Khim-Term Obrab Stali Splavov 6 (1969) 129.

[22] A.V. Tomilov, G.V. Shcherbedinskii, Fiz. Khim. Met. Mater. 3 (1967) 261.

[23] R. Kirchner, Nucl. Instr. and Meth. B 26 (1987) 204.